PB88-170683

Fourier Transform Infrared Photoacoustic Spectroscopy Characterization of Sulfur-Oxygen Species Resulting from the Reaction of SO2 with CAO and CaCO3

Duke Univ., Durham, NC

Prepared for

Environmental Protection Agency
Research Triangle Park, NC

1987

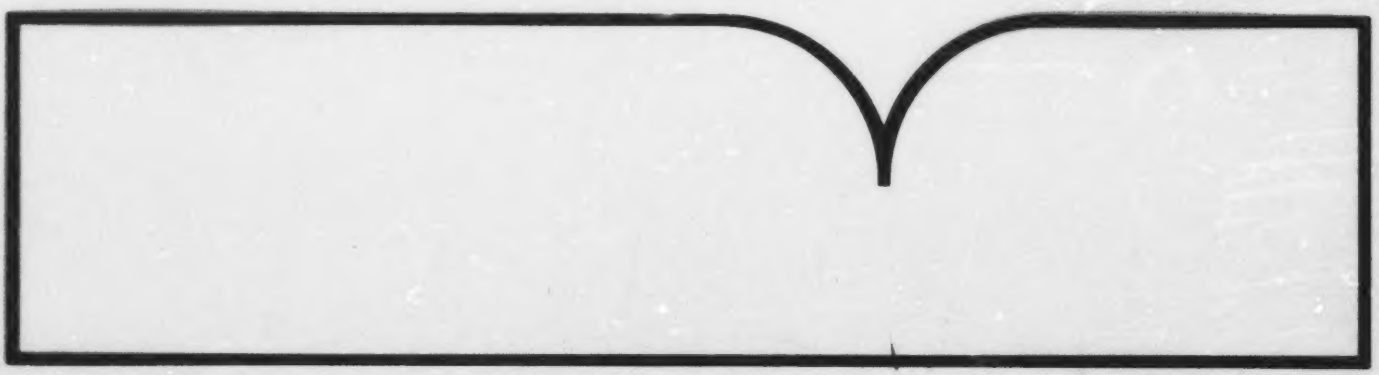

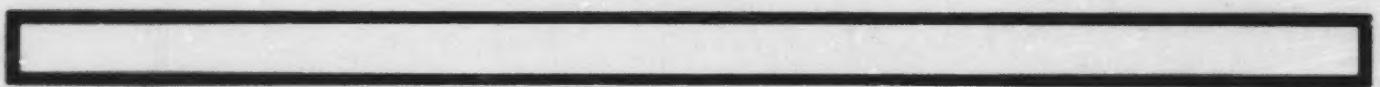

U.S. Department of Commerce
National Technical Information Service
NTIS

TECHNICAL REPORT DATA
(Please read Instructions on the reverse before completing)

1. REPORT NO. EPA/600/J-87/227	2.
3. RE PB88-170683	
4. TITLE AND SUBTITLE Fourier Transform Infrared Photoacoustic Spectroscopy Characterization of Sulfur-Oxygen Species Resulting from the Reaction of SO_2 with CaO and $CaCO_3$ (Journal Version)	5. REPORT DATE 1987
	6. PERFORMING ORGANIZATION CODE
7. AUTHOR(S) Meg A. Martin, Jeffrey W. Childers, and Richard A. Palmer	8. PERFORMING ORGANIZATION REPORT NO.
9. PERFORMING ORGANIZATION NAME AND ADDRESS Duke University, P. M. Gross Chemistry Laboratory, Durham, North Carolina 27706	10. PROGRAM ELEMENT NO.
	11. CONTRACT/GRANT NO. Cooperative Agreement CR811629
12. SPONSORING AGENCY NAME AND ADDRESS EPA, Office of Research and Development, Air and Energy Engineering Research Laboratory, Research Triangle Park, NC 27711	13. TYPE OF REPORT AND PERIOD COVERED Journal Article; 1/85-1/86
	14. SPONSORING AGENCY CODE EPA/600/13

15. SUPPLEMENTARY NOTES AEERL project officer is Merrill D. Jackson, Mail Drop 62, 919/541-2559. Applied Spectroscopy, Vol. 41, No. 1, pp. 120-126 (1987).

16. ABSTRACT Fourier transform infrared photoacoustic spectroscopy (FTIR-PAS) has been used to investigate the reaction of SO2 in He with CaO and CaCO3 particles at temperatures between 25 and 900 C. SO2 reacts with CaC at 25 C, while the reaction of CaCO3 with SO2 is first evident at 550 C (the initial product of both reactions is CaSO3). The CaSO3 then further reacts with SO2 to form CaSO4, CaS2O3, and CaS at higher temperatures. At 900 C and above, the net production of SO4(--) and S2O3(--) is decreased due to the decomposition of SO3(--). FTIR-PAS depth profiling experiments indicate the formation of a reaction-limiting product layer of SO3(--) and SO4(--) from the above reactions on the surface of the CaO and CaCO3 particles.

17. KEY WORDS AND DOCUMENT ANALYSIS

a. DESCRIPTORS		b. IDENTIFIERS/OPEN ENDED TERMS	c. COSATI Field/Group
Pollution	Calcium Oxides	Pollution Control	13B
Fourier Transformation	Calcium Carbonates	Stationary Sources	12A
Infrared Spectroscopy		Photoacoustic Spectroscopy	14B
Acoustic Measurement	Desulfurization		20A 07A, 07D
Photometry	Analyzing	FTIR-PAS	
Sulfur Dioxide			07B

18. DISTRIBUTION STATEMENT Release to Public	19. SECURITY CLASS (This Report) Unclassified	21. NO. OF PAGES 9
	20. SECURITY CLASS (This page) Unclassified	22. PRICE PC 9.95 / MF A6.95

EPA Form 2220-1 (9-73)

REPRODUCED BY
U.S. DEPARTMENT OF COMMERCE
NATIONAL TECHNICAL
INFORMATION SERVICE
SPRINGFIELD, VA. 22161

EPA/600/J-87/227
JOURNAL ARTICLE

Fourier Transform Infrared Photoacoustic Spectroscopy Characterization of Sulfur-Oxygen Species Resulting from the Reaction of SO_2 with CaO and $CaCO_3$

MEG A. MARTIN, JEFFREY W. CHILDERS, and RICHARD A. PALMER*
P. M. Gross Chemistry Laboratory, Duke University, Durham, North Carolina 27706

Fourier transform infrared photoacoustic spectroscopy (FT-IR/PAS) has been used to investigate the reaction of SO_2 in He with CaO and $CaCO_3$ particles at temperatures between 25 and 900°C. The reaction of SO_2 with CaO occurs at 25°C, while the reaction of $CaCO_3$ with SO_2 is first evident at 550°C. The initial product of both of these reactions is $CaSO_3$. The $CaSO_3$ then further reacts with SO_2 to form $CaSO_4$, CaS_2O_3, and CaS at higher temperatures. At 900°C and above, the net production of $SO_4^{=}$ and $S_2O_3^{=}$ is decreased because of the decomposition of $SO_3^{=}$. FT-IR/PAS depth-profiling experiments indicate the formation of a reaction-limiting product layer of $SO_3^{=}$ and $SO_4^{=}$ from the above reactions on the surface of the CaO and $CaCO_3$ particles.

Index Headings: Fourier transform infrared spectroscopy; Photoacoustic spectroscopy; Analysis for sulfur-oxygen groups; Desulfurization processes.

INTRODUCTION

Methods currently under investigation for reducing SO_2 emissions from power plants and other stationary sources of air pollution include several processes based on the use of solid alkali sorbents. For example, in dry injection processes, materials such as finely ground limestone are blown into the furnace within and above the combustion zone. Several studies of the fundamental thermodynamics and the kinetics of the reactions involved in this type of stack gas scrubbing have been reported.[1-7] In order to develop the most efficient, economical, and practical SO_2 scrubbing methods it is important to be able to analyze the reaction products resulting from evaluative experiments quickly and with an absolute minimum of disturbance of the samples, so as to avoid intervening secondary reactions. In addition, methods of analysis should be applicable to reaction conditions and sorbent characteristics which approximate as closely as possible those in practical applications.

Previous efforts to characterize the reaction of SO_2 with alkali sorbents have failed to meet one or more of the above criteria in that they have, for example, involved spectroscopic studies of sorbents deposited on substrates or the use of wet chemical analysis of particulate products for total SO_2 conversion. In the work reported here, Fourier transform infrared spectrometry with photoacoustic detection (FT-IR/PAS) has been evaluated for application to this problem. FT-IR/PAS combines the speed of spectrometric analysis with the ability of the photoacoustic technique to detect light absorption on a wide range of particulate samples in the "as received" state. PAS is capable of providing qualitative and quantitative data on many optically opaque and/or highly scattering materials with little or no sample preparation. In addition, photoacoustic detection is capable of distinguishing between surface (or near-surface) and bulk chromophores and is less susceptible to signal saturation effects than are other detection techniques such as IR transmission and diffuse reflectance spectrometry.[8] These characteristics of FT-IR/PAS make it well suited for the study of heterogeneous reactions such as those of gaseous SO_2 with finely divided solids.

The emphasis of this investigation is to demonstrate the spectroanalytical capabilities of FT-IR/PAS to characterize the products of the reaction of SO_2 with powdered alkali sorbents; e.g., $CaCO_3$ and CaO. The conditions chosen are intended not to mimic actual smokestack conditions or to approximate any particular scrubbing methodology, but to provide a well-characterized and controlled test of the spectroanalytical method as applied to relevant as-received particulate samples.

EXPERIMENTAL

Chemicals. Powdered samples of CaO (99.999% Aldrich Gold Label) and $CaCO_3$ (Fisher Reagent) were used as reactive sorbents. Prior to reaction, we sieved these materials to obtain a particle size range of 50 to 100 μm. Sample sizes were 40 mg for CaO and 80 mg for $CaCO_3$. Certified standard 1.5% SO_2 in helium (99.98% SO_2, 99.995% He; Matheson) was used as the exposure gas. For reactions of SO_2 with CaO, the SO_2 gas mixture was diluted to 0.75% SO_2 with helium (99.997% He; National Welders). The helium was passed through a drying column (Alltech) prior to use.

Exposure Procedure. The solid-gas reaction of these materials was studied under various conditions of temperature and exposure time. For a typical experiment, samples were weighed under an inert atmosphere of helium and placed on a quartz frit at the center of a 60-cm-long quartz reaction tube. This tube was then sealed by Teflon® valves at both ends and connected to the stainless-steel tubing of the gas delivery system. The reaction tube was then positioned in the bore of a vertically mounted Lindberg Model 53035 tube furnace. The furnace temperature was monitored by an internal thermocouple. Once the sample was positioned in the preheated tube furnace it was exposed to the reaction gas for a predetermined time at the desired gas flow rate. At the end of the exposure time the reaction tube was flushed with helium, immediately removed from the furnace, and allowed to cool to ambient temperature while

Received 27 May 1986.
* Author to whom correspondence should be sent.

0003-7028/87/4101-0120$2.00/0
© 1987 Society for Applied Spectroscopy
NTIS is authorized to reproduce and sell this report. Permission for further reproduction must be obtained from the copyright owner.

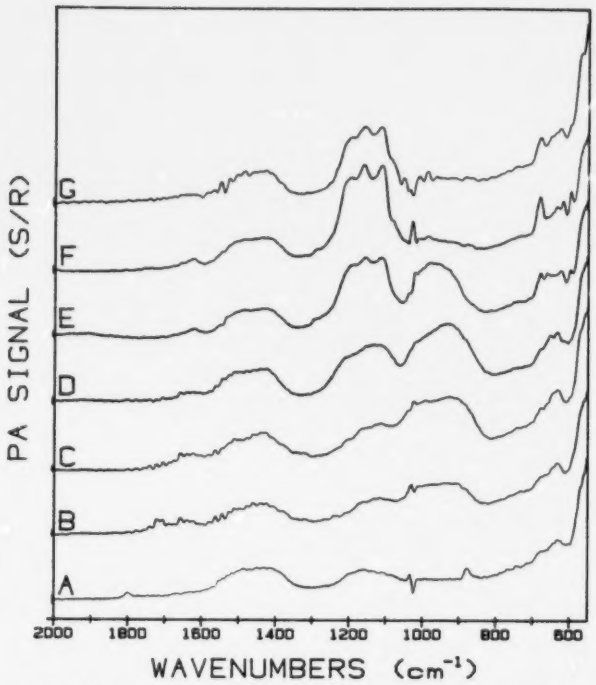

FIG. 1. FT-IR/PAS of CaO (A); exposed to 0.75% SO_2 in He for 10 min at 25°C (B), 200°C (C), 400°C (D), 550°C (E), 750°C (F), 900°C (G).

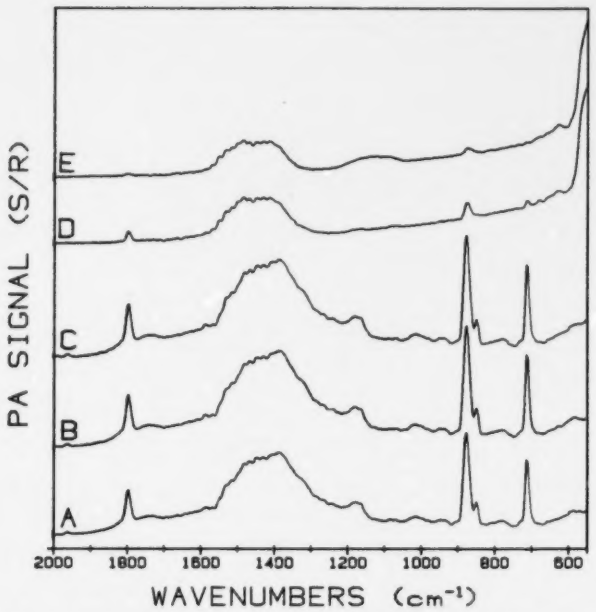

FIG. 2. FT-IR/PAS of $CaCO_3$ (A); heated under He for 30 min at 350°C (B), 550°C (C), 750°C (D), 900°C (E).

still being flushed with dry helium. (The cooling period was at most 7 min.) The reaction tube was then resealed, disconnected from the gas delivery system, and transferred to a helium-filled glove bag in which the sample was loaded into the photoacoustic accessory. The PAS cell was then positioned in the sample compartment of the Fourier transform infrared spectrometer for spectral measurements within 10 min of sample loading.

Spectral Measurements. The IBM Instruments Photoacoustic Accessory (Model A6120890) is equipped with an internal preamplifier,[9] and the resulting output of the photoacoustic cell is fed directly into the signal input of the IBM 91/95 FT-IR spectrometer electronics. Spectra were normally acquired with the use of 8 cm^{-1} resolution and a mirror velocity of 0.059 cm/s (optical velocity, 0.235 cm/s), yielding maximum Fourier frequencies of 129 to 470 Hz over the range of 550 to 2000 cm^{-1}. For "depth profiling" experiments, the mirror velocity was incrementally increased from 0.059 to 0.333 cm/s (optical velocity, 1.332 cm/s), yielding maximum Fourier frequencies of 732 to 2664 Hz over the same spectral range. Standard measurements were made with 128 to 512 co-added interferograms transformed with the Cooley-Tukey fast Fourier transform and Happ-Genzel apodization. We normalized all FT-IR/PA spectra to the corresponding spectrum of Norit-A carbon black to remove any spectral structure due to the light source and optics. In terms of band shape and position, the photoacoustic spectra are equivalent to absorption curves (provided the thermal saturation limit is not exceeded).[8] Peak amplitudes or areas may be calibrated with the use of standard procedures so that quantitative analyses may be obtained. In this work, we used standard gravimetric methods for $SO_4^=$ when necessary, to calibrate and verify the spectral results.

RESULTS AND DISCUSSION

Reaction of CaO with SO_2. Figure 1 depicts the spectral data obtained for replicate 40-mg samples of CaO exposed to 0.75% SO_2 in helium for 10 min at successively higher temperatures. The flow rate of gas used was 6 mL/min. Trace A of Fig. 1 is a typical spectrum of CaO (containing residual amounts of carbonate as indicated by the broad band centered at ~1450 cm^{-1} characteristic of the ν_3 C-O stretching mode). Trace B (Fig. 1) shows the presence of a broad band centered at ~950 cm^{-1} after exposure of the sample to SO_2 at 25°C. When the sample is exposed to increasing amounts of SO_2 at 25°C, the broad absorption centered at 950 cm^{-1} increases and a shoulder at 630 cm^{-1} becomes evident. These bands are characteristic of those reported in the literature for $SO_3^=$.[10] The band at 950 cm^{-1} is assigned to the ν_1 and ν_3 symmetric and asymmetric S-O stretching modes, respectively. The shoulder at 630 cm^{-1} is characteristic of the ν_2 symmetric bending mode. Nyberg and Larsson[11] determined that low frequencies of ν_1 and ν_3 (<1000 cm^{-1}) are characteristic of coordination of the $SO_3^=$ to the metal through an oxygen. These data then indicate that SO_2 binds to the oxygen on the CaO surface as the initial reaction product $SO_3^=$ is formed. This conclusion contrasts with a previous interpretation in which Low *et al.*[7] attributed a trio of bands at 973, 925, and 632 cm^{-1} to a pyramidal sulfite-ion product bound to the CaO surface through the sulfur. However, a study of thiosulfates by Freedman and Straughan[12] further supports Nyberg and Larsson's conclusions and, on the basis of these considerations, the bands are assigned to binding of SO_2 through $O^=$ to Ca^{++}, effectively forming surface-bound $SO_3^=$.

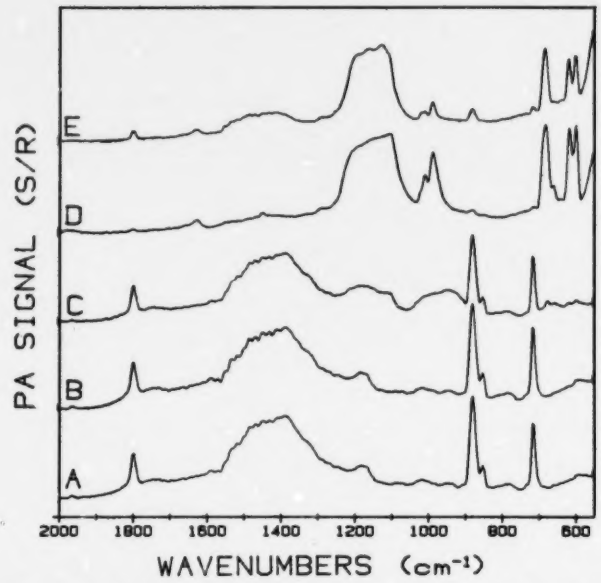

FIG. 3. FT-IR/PAS of $CaCO_3$ (A); exposed to 1.5% SO_2 in He for 30 min at 350°C (B), 550°C (C), 750°C (D), 900°C (E).

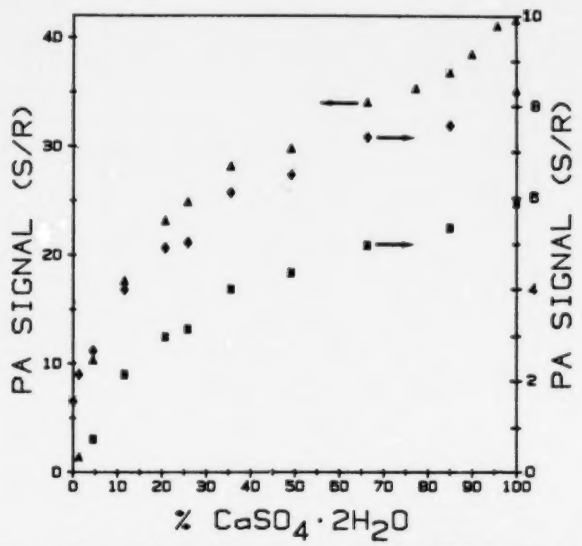

FIG. 4. Plot of PA signal intensity vs. % $CaSO_4 \cdot 2H_2O$ by weight in $CaSO_4 \cdot 2H_2O$:$CaCO_3$ physical mixtures. (▲) 1153 cm^{-1}; (■) 679 cm^{-1}; (◆) 610 cm^{-1}.

After exposure of a CaO sample to SO_2 for 10 min at 200°C (Trace C, Fig. 1), the band at 950 cm^{-1} shows increased intensity. For exposures at 400°C (Trace D), a third additional band is observed at 1153 cm^{-1}. Also, several subtle changes in the 700–600 cm^{-1} region of the spectrum are observed. The broad band at 1153 cm^{-1} is attributed to amorphous sulfate formed by the reaction of surface-bound sulfite and additional SO_2 (see below). Also, after the 400°C exposure, the sulfite band at 950 cm^{-1} shows increased intensity, and the ν_3 asymmetric stretching mode maximum shifts to higher energy. Trace E of Fig. 1 (550°C exposure) exhibits increased intensity of the 1153-cm^{-1} sulfate band, which splits into three components at 1157, 1130, and 1080 cm^{-1}. In addition, three small peaks at 679, 613, and 594 cm^{-1} are observed. All six bands at 1157, 1130, 1080, 679, 613, and 594 cm^{-1} are assigned to the ν_3 stretching and ν_4 bending modes of bidentate $SO_4^{=}$.[13] In Trace F of Fig. 1, the spectrum of a sample of CaO exposed to SO_2 at 750°C shows more pronounced absorption for the split 1153-cm^{-1} band and for the peaks at 679, 613, and 594 cm^{-1}. In addition, a sharp peak is observed at 1011 cm^{-1}, which is assigned to the ν_1 (symmetric stretch) mode of $SO_4^{=}$. This sample shows virtually no evidence of $SO_3^{=}$. For the 900°C exposure (Trace G, Fig. 1), the broad band at 1153 cm^{-1} and peaks at 679, 613, and 594 cm^{-1} show decreased intensities. Several small peaks and a shoulder appear just below the 1153 cm^{-1} peak. These peaks indicate the presence of species of the general formula $S_xO_y^{-n}$ which result from the decomposition of $SO_3^{=}$ and $SO_4^{=}$ and subsequent polymerization of their products.[7,14,15]

Reaction of $CaCO_3$ with SO_2. Figure 2 illustrates the result of heating $CaCO_3$ under pure He for 30 min at various temperatures. Trace A of Fig. 2 is the spectrum of pure $CaCO_3$. The broad band at 1450 cm^{-1} and sharp peaks at 876 and 714 cm^{-1} are assigned to the ν_3, ν_2, and ν_4 modes of $CO_3^{=}$, respectively. In addition there is a band at 1784 cm^{-1}, which is assigned to the $(\nu_1 + \nu_4)$ combination mode.[16] Traces B and C (Fig. 2), spectra of samples heated at 350 and 550°C, respectively, exhibit identical spectral features. However, the sample heated at 750°C (Trace D) shows extensive loss of band intensity at 1450, 876, and 714 cm^{-1}. This is indicative of the calcination process, in which CO_2 is released from the crystalline $CaCO_3$ structure. It is interesting to note that residual carbonate remains in the sample even after heating for 30 min at 900°C (Trace E).

Figure 3 illustrates the spectral data obtained from replicate samples of $CaCO_3$ exposed to 1.5% SO_2 in helium for 30 min at successively higher temperatures. The reaction of SO_2 with $CaCO_3$ is first evident for exposures above 350°C (Trace B, Fig. 3). At 550°C (Trace C), broad bands are observed at 950 and 1153 cm^{-1}. As before, these bands are assigned to $SO_3^{=}$ and $SO_4^{=}$ species, respectively.

The exposure of $CaCO_3$ to 1.5% SO_2 in helium at 750°C (Trace D, Fig. 3) produces a sample with spectral bands at 1153, 1003, 984, 679, 656, 613, and 594 cm^{-1}. The first group of bands at 1153, 679, 613, and 594 cm^{-1} is assigned to bidentate sulfate (see above). The second group of bands at 1003, 984, and 656 cm^{-1} is attributed to surface thiosulfate. The bands at 1003, 984, and 656 cm^{-1} correspond to the ν_1, ν_3 (symmetric stretch), and ν_2 (symmetric bend) thiosulfate modes, respectively. Freedman and Straughan[12] studied a number of ionic thiosulfates in order to establish reliable criteria from the IR data to determine the type of coordination of the thiosulfate to the metal. They determined that the ν_1 and the ν_3 frequencies are reliable indicators of the type of thiosulfate coordination. The ν_1 and ν_3 frequencies in this case are indicative of oxygen coordination of the thiosulfate to a metal.

After exposure at 900°C (Trace E, Fig. 3), the bands at 1003, 984, and 656 cm^{-1} are clearly less intense than

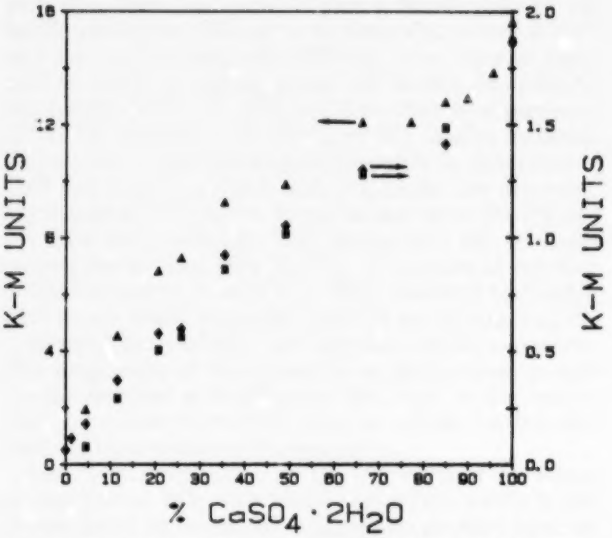

FIG. 5. Plot of Kubelka-Munk function vs. % $CaSO_4 \cdot 2H_2O$ in $CaSO_4 \cdot 2H_2O$:$CaCO_3$ physical mixtures. (▲) 1153 cm^{-1}; (■) 679 cm^{-1}; (◆) 610 cm^{-1}.

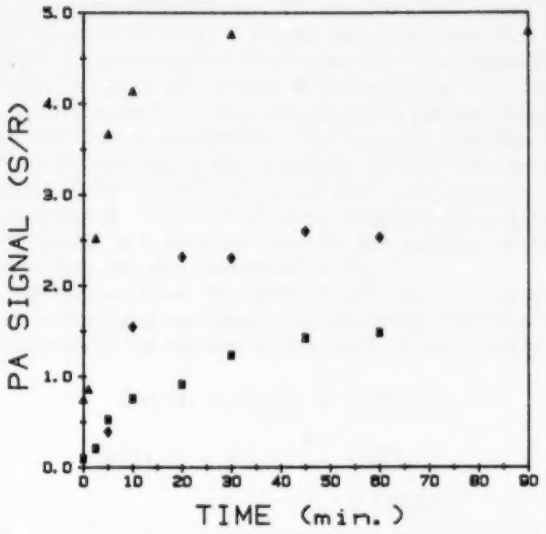

FIG. 6. Peak areas of $\nu_{1,3}$ SO_3^- (950 cm^{-1}) formed from the reaction of 0.75% SO_2 in He with CaO at 25°C (▲); ν_4 SO_4^- (679 cm^{-1}) formed from the reaction of 0.75% SO_2 in He with CaO at 750°C (■); ν_4 SO_4^- (679 cm^{-1}) formed from the reaction of $CaCO_3$ with 1.5% SO_2 in He at 750°C (◆).

after exposure at 750°C. The sulfate bands at 1153, 679, 613, and 594 cm^{-1} are also lower in intensity compared with those formed during the 750°C exposure of $CaCO_3$ to SO_2.

Depth Profile Experiments. For these experiments the FT-IR/PA data are used to quantify the extent of reaction of SO_2 with CaO and $CaCO_3$. It is therefore important to show that the FT-IR/PA signal is not photothermally saturated. In order to test for saturation, we have plotted the photoacoustic peak areas of sulfate bands at 1153, 679, and 610 cm^{-1} as a function of concentration of $CaSO_4 \cdot 2H_2O$ mixed with $CaCO_3$ (Fig. 4). The powders were first ground and sieved separately, providing a particle size between 50 and 100 μm. We then mixed the $CaSO_4 \cdot 2H_2O$ and $CaCO_3$ by shaking them for one minute with a Wig-L-Bug (Crescent Dental Manufacturing Co.), which we used without the grinding ball so as to avoid further particle-size reduction. The nonlinear dependence of the photoacoustic signal on sulfate concentration for the three sulfate bands can be attributed to either signal saturation at high concentrations or light scattering effects which enhance the PA signal at low concentrations. In order that a distinction between these two effects could be made, the PA data were subjected to a Kubelka-Munk analysis.[17]

Freeman *et al.*[18] noted that the PA signal is quite analogous to the diffuse reflectance response for a scattering solid sample. They suggested that, if a sample was illuminated by diffuse light and if the sample was sufficiently thick to be optically opaque, the PA signal could be analyzed with the use of the Kubelka-Munk function. In fact, linear relationships between UV-VIS PA data treated with the Kubelka-Munk function and concentration have recently been reported.[19,20] The results of such an analysis of the data from the $CaSO_4 \cdot 2H_2O$/$CaCO_3$ series are shown in Fig. 5. The nonlinear dependence of the 1153 cm^{-1} band intensity indicates that this band is photothermally saturated and therefore inappropriate for quantitative sulfate determinations. On the other hand, the linearity of the 679 and 610 cm^{-1} band intensities vs. concentration plots shows that these bands are not saturated, even for the pure sulfate, and can thus be used as indicators for the extent of reaction in SO_2 exposure experiments.

For the conditions of these experiments, the FT-IR/PA data for both the CaO and $CaCO_3$ samples indicate limits to their reactivity with SO_2 during the formation

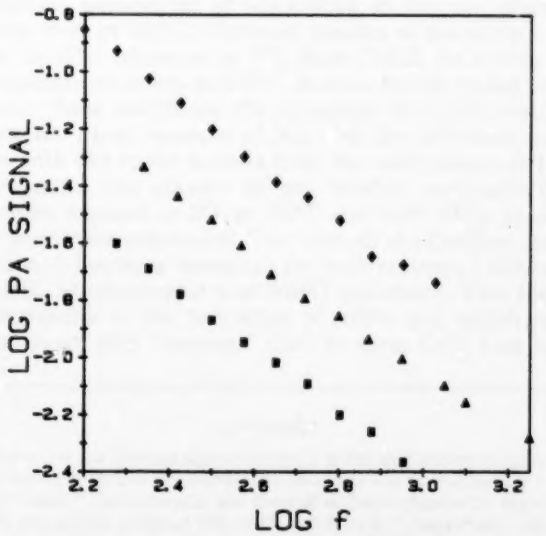

FIG. 7. Photothermal modulation frequency dependence of IR band intensities. CaO exposed to 0.75% SO_2 in He at 750°C, ν_4 SO_4^- (679 cm^{-1}) (▲); $CaCO_3$ exposed to 1.5% SO_2 in He at 750°C, ν_4 SO_4^- (679 cm^{-1}) (■); CaO exposed to 0.75% SO_2 in He at 25°C, $\nu_{1,3}$ SO_3^- (950 cm^{-1}) (◆).

of sulfite at 25°C as well as for the formation of sulfate and thiosulfate at 750°C. Figure 6 shows plots of the sulfite peak area (950 cm^{-1}) vs. time of exposure at 25°C and the sulfate peak area (679 cm^{-1}) vs. time of exposure at 750°C, for exposures of CaO to SO_2. In addition, the sulfate peak area (679 cm^{-1}) vs. time of exposure at 750°C for exposures of $CaCO_3$ to SO_2 is also depicted. These plots clearly show the differences in capacities of CaO and $CaCO_3$ to react with SO_2 under the described experimental conditions. It can be seen from the FT-IR/PA data that, although CaO reacts with SO_2 at lower temperatures than does $CaCO_3$, the extent of reaction of CaO is only *ca.* one third of that exhibited by $CaCO_3$. This is especially apparent through examination of the ν_4 spectral band of $SO_4^=$ for CaO and $CaCO_3$ exposures. The magnitude of the ν_4 band is *ca.* three times greater for the reaction of $CaCO_3$ with SO_2 than in the case of CaO. Gravimetric analysis data for sulfate confirm this spectral observation and conclusion.

The most likely reason for this limitation of the extent of reaction of SO_2 with these particulate solids is the formation of an essentially impervious product layer on the surface of the particles. If this is so and if a nominal particle diameter of 100 μm is assumed, then the thickness of this layer can be estimated to be on the order of 2 μm for CaO and 7 μm for $CaCO_3$. This is based on the percent conversion of $CO_3^=$ to $SO_4^=$ determined by wet chemistry in each case, ignoring differences in anion volume. This product-layer model is supported by the results of photothermal depth profiling experiments as described below.

Figure 7 shows the modulation frequency dependence of the photoacoustic signal amplitude of the 679 cm^{-1} band of sulfate formed from the reaction of 0.75% SO_2 in helium with particulate CaO at 750°C for 10 min. The log-log plot of amplitude vs. frequency has a slope of -1.10 ± 0.01 for modulation (Fourier) frequencies of 160 to 2200 Hz (for 679 cm^{-1}). From an estimate of the thermal diffusion depth of CaO for 2200 Hz and the fact that this band does not exhibit photothermal saturation at this frequency, even in pure $CaSO_4$, the *optical* absorption depth can be estimated to be greater than 100 μm at 679 cm^{-1}. That means that for particles of pure $CaSO_4$ of diameter 100 μm, the optical absorption length is greater than the particle diameter. The modulation frequency dependence of ~ -1 then indicates that the chromophoric material ($CaSO_4$) must be distributed in a layer which extends, from the surface, no deeper than the thermal diffusion depth, even for the highest modulation frequency used (estimated to be ~16 μm for a $CaSO_4$-like solid at 2200 Hz). If the product were distributed uniformly throughout the particle (unlikely) or if the layer were thicker than this minimum thermal diffusion depth, then the slope of the log-log plot in Fig. 7 would be expected to be −1.5, in the first instance, or to change from −1 to −1.5 for higher modulation frequencies, in the second instance.†

An identical analysis to that above can be applied to the exposure of $CaCO_3$ to 1.5% SO_2 at 750°C, using the $SO_4^=$ band at 679 cm^{-1}. These data show that this reaction is also limited by the formation of an impervious product layer on the surface of the particles. Data from samples exposed at lower temperatures are also consistent with this interpretation. For example, with the use of the nonsaturating $SO_3^=$ band at 950 cm^{-1} for an exposure of CaO to 0.75% SO_2 at 25°C, the slope of the log-log plot is -1.04 ± 0.02, indicating that this reaction also results in a product layer on the particle surface. These data are also illustrated in Fig. 7.

Mechanism. From the above data it can be concluded that under these conditions the following reactions are important in the capture of SO_2 by CaO and $CaCO_3$:

$$CaO(s) + SO_2(g) \xrightarrow{25°C} CaSO_3(s), \quad (1)$$

$$CaCO_3(s) + SO_2(g) \xrightarrow{550°C} CaSO_3(s) + CO_2(g), \quad (2)$$

$$2CaSO_3(s) + SO_2(g) \xrightarrow{750°C} 2CaSO_4(s) + \tfrac{1}{2}S_2(g), \quad (3)$$

$$4CaSO_3(s) \xrightarrow{750°C} 2CaSO_4(s) + CaS_2O_3(s) + CaO(s). \quad (4)$$

The ways in which the solid surface might promote these reactions are schematically illustrated in Fig. 8.

Reaction 1, the reaction of SO_2 with CaO, results in the production of $CaSO_3$ for temperatures between 25 and 550°C. Reaction 2 illustrates the reaction of SO_2 with $CaCO_3$. This reaction occurs at 550°C and above. It is interesting to note that (in pure He) calcination is observed only for temperatures *above* 550°C (Fig. 2). In addition, calcination of the $CaCO_3$ in He was incomplete, even at 900°C. However, spectra of the sample of $CaCO_3$ after exposure to SO_2 show $CaSO_3$ formation at temperatures as low as 550°C. It must be concluded that under these conditions the formation of $CaSO_3$ results from the direct reaction of SO_2 with the carbonate and not with the oxide formed from the calcination of the carbonate. The absence of any residual carbonate for samples exposed to SO_2 at 750°C and 900°C (Fig. 3) also supports this conclusion. The formation of sulfate (Reaction 3) becomes dominant for both systems, CaO and $CaCO_3$, at temperatures of 550°C and above. This reaction results in the formation of sulfur gas, which can then react with "nascent" CaO to form CaS. CaS has

† The thermal dependence of the photothermal signal gives rise to the possibility of using PAS for probing the subsurface structure of heterogeneous samples. This is because only the light absorbed in a thermally active layer below the illuminated surface can contribute to the signal. This layer thickness is defined as

$$\mu_s = (\alpha/\pi f)^{1/2}$$

where α is the thermal diffusivity and f is the modulation frequency in Hz.[21] For sulfate and sulfite-like materials α is approximately 1×10^{-3} cm/s.[22] Consequently, the thermal diffusion depths for the sulfite and sulfate peaks at 980, 1153, and 610 cm^{-1} range from ~40 to 10 μm for Fourier frequencies from 160 to 2200 Hz. At these wavenumbers the CaO and $CaCO_3$ substrates are themselves transparent (i.e., the optical absorption depth is greater than the particle thickness).

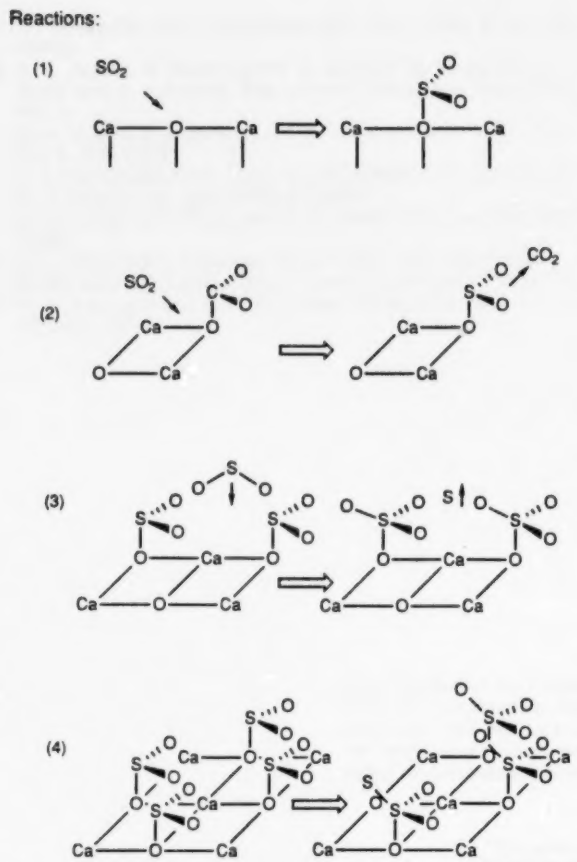

FIG. 8. Schematic illustrations of proposed mechanisms for the reaction of SO_2 with CaO and $CaCO_3$.

been confirmed in such samples by qualitative wet chemical analysis.

Another possible route to $SO_4^=$ in the absence of oxygen is the disproportionation of $SO_3^=$:

$$4CaSO_3(s) \rightarrow 3CaSO_4(s) + CaS(s). \quad (5)$$

Foerster and Kubel[14] showed that this reaction becomes spontaneous above 650°C. However, in the reactions reported here it appears that this path is relatively unimportant. This is supported by the results of experiments illustrated in Fig. 9. Trace A, Fig. 9 is the spectrum of a CaO sample exposed to SO_2 (0.75%) at 25°C for 10 min. A replicate sample was exposed at 25°C and then heated under pure He for 10 min at 750°C to yield Trace B; a third sample was *exposed* for 10 min *at* 750°C, to yield Trace C. Clearly very little $SO_3^=$ is converted by simple disproportionation relative to that created by reaction with additional SO_2 (pseudo-disproportionation).

However, when the reaction is more extensive, as is particularly so in the case of $CaCO_3$ exposed at 750°C, a third route to $SO_4^=$ is revealed. This is the disproportionation to thiosulfate (Reaction 4). Thiosulfate is identified in the product from distinctive bands at 1003, 984, and 656 cm^{-1} (Fig. 3). Although the presence of $S_2O_3^=$ is clear in samples of $CaCO_3$ exposed at 750°C, it is virtually absent in samples after exposure at 900°C. Thiosulfate has not been detected in samples of CaO

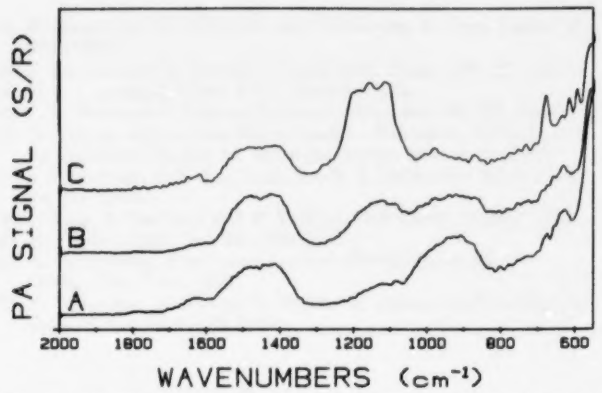

FIG. 9. FT-IR/PAS of CaO exposed to 0.75% SO_2 in He at 25°C for 10 min (A), then heated in He at 750°C for 10 min (B), and exposed to 0.75% SO_2 in He at 750°C for 10 min (C).

exposed at 750°C, but this may be due to the lower total SO_2-capture by the CaO particles.

SUMMARY

Under the conditions of this experiment (~50 μm particles exposed to low concentrations of SO_2 in an inert carrier gas for 1 to 60 min), calcium oxide reacts rapidly, even at ambient temperature, while the carbonate only reacts appreciably at 550°C and above. By use of photoacoustic detection of the infrared spectra of the exposed powder as received, it is clear that the initial product in either case is calcium sulfite and that, at temperatures above 550°C, further reaction with SO_2 and/or disproportionation lead to the production of sulfate, thiosulfate, and sulfide. The PAS results coupled with wet chemical analysis show that the reaction with both CaO and $CaCO_3$ is limited by the formation of an impervious product layer on the particle surface, and that this layer is essentially completely converted to $SO_4^=$ at temperatures of 750°C and above. The spectral results also show that the extent of reaction on these relatively large particles is *ca.* three times greater for the carbonate than the oxide and that for either substrate capture of SO_2 is less at 900° than at 750°C, apparently because of the decomposition of $SO_3^=$ at the higher temperatures.

ACKNOWLEDGMENTS

Support by Cooperative Agreement CR-811629-01-0 (Project Officer, Merrill Jackson) from the Environmental Protection Agency is gratefully acknowledged. Although the research was funded by the U.S.E.P.A., it has not been subjected to full Agency review and therefore does not necessarily reflect the views of the Agency and no official endorsement should be inferred. Donation of equipment, by Dr. Riley S. Stallings, is also gratefully acknowledged.

1. R. H. Borgwardt, K. R. Bruce, and J. Blake, *Proceedings: First Joint Symposium on Dry SO_2 and Simultaneous SO_2/NO_x Control Technologies*, EPA-600/9-85-020a (NTIS) (PB85-232353) (U.S. Environmental Protection Agency and the Electric Power Research Institute, San Diego, California, 1984), Vol. 1.
2. R. H. Borgwardt, Environ. Sci. Technol. **4**, 59 (1970).
3. G. Van Houte and B. Delmon, Bull. Soc. Chim. Belg. **87**, 241 (1978).
4. G. Van Houte and B. Delmon, J. Chem. Soc., Faraday Trans. 1, **75**, 1593 (1979).

5. T. Tarradellas and L. Bonnetain, Bull. Soc. Chim. Fr. **6**, 1903 (1973).
6. J. S. Burton, in *Developments In Applied Spectroscopy*, E. L. Grove and A. J. Perkins, Eds. (Plenum Press, New York, 1971), Vol. 9.
7. M. J. D. Low, A. J. Goodsel, and N. Takeawa, Environ. Sci. Technol. **5**, 1191 (1971).
8. J. F. McClelland, Anal. Chem. **55**, 89A (1983); J. W. Childers and R. A. Palmer, Am. Lab. **18(3)**, 22 (1986).
9. D. J. Gerson, J. S. Wong, and J. M. Casper, Am. Lab. **16(11)**, 63 (1984).
10. J. C. Evans and J. Bernstein, Can. J. Chem. **33**, 1270 (1955).
11. B. Nyberg and R. Larsson, Acta Chemica Scandinavia **27**, 63 (1973).
12. A. N. Freedman and B. P. Straughan, Spectrochim. Acta, Part A, **27**, 1455 (1971).
13. E. Steger and W. Schmidt, Ber. Bunsenges. J. Phys. Chem. **68**, 102 (1964).
14. F. Foerster and K. Kubel, Z. Anorg. Allg. Chem. **139**, 261 (1924).
15. G. J. Marchal, J. Chim. Phys. **22**, 413 (1925).
16. S. D. Ross and J. Goldsmith, Spectrochim. Acta **20**, 781 (1964).
17. G. Kortüm, *Reflectance Spectroscopy—Principles, Methods, and Applications*, English ed. (Springer-Verlag, New York, 1969).
18. J. J. Freeman, R. M. Friedman, and H. S. Reichard, J. Phys. Chem. **84**, 315 (1980).
19. D. King, R. Davidson, and M. Phillips, Anal. Chem. **54**, 2191 (1982).
20. R. Tilgner, Appl. Opt. **20**, 3780 (1981).
21. A. Rosencwaig, *Photoacoustics and Photoacoustic Spectroscopy* (Wiley, New York, 1980).
22. Y. Yokoyama, M. Kosugi, H. Kanda, M. Ozasa, and K. Hodouchi, Bunseki Kagaku **33**, E1 (1984).

NOTICE

This document has been reviewed in accordance with U.S. Environmental Protection Agency policy and approved for publication. Mention of trade names or commercial products does not constitute endorsement or recommendation for use.

This article documents research that was conducted under the auspices of the U.S. Environmental Protection Agency (USEPA). As an arm of the government, the USEPA has a paid up, non-exclusive, irrevocable, worldwide license to reproduce, prepare derivative works, and distribute to the public all of the material contained herein, and to grant others acting on its behalf the right to do so. The USEPA grants to the National Technical Information Service, Department of Commerce, the right to act as its agent in the distribution of this material.